

UEL 340 Des biomatériaux à l'ingénierie tissulaire

Analyse de Surface

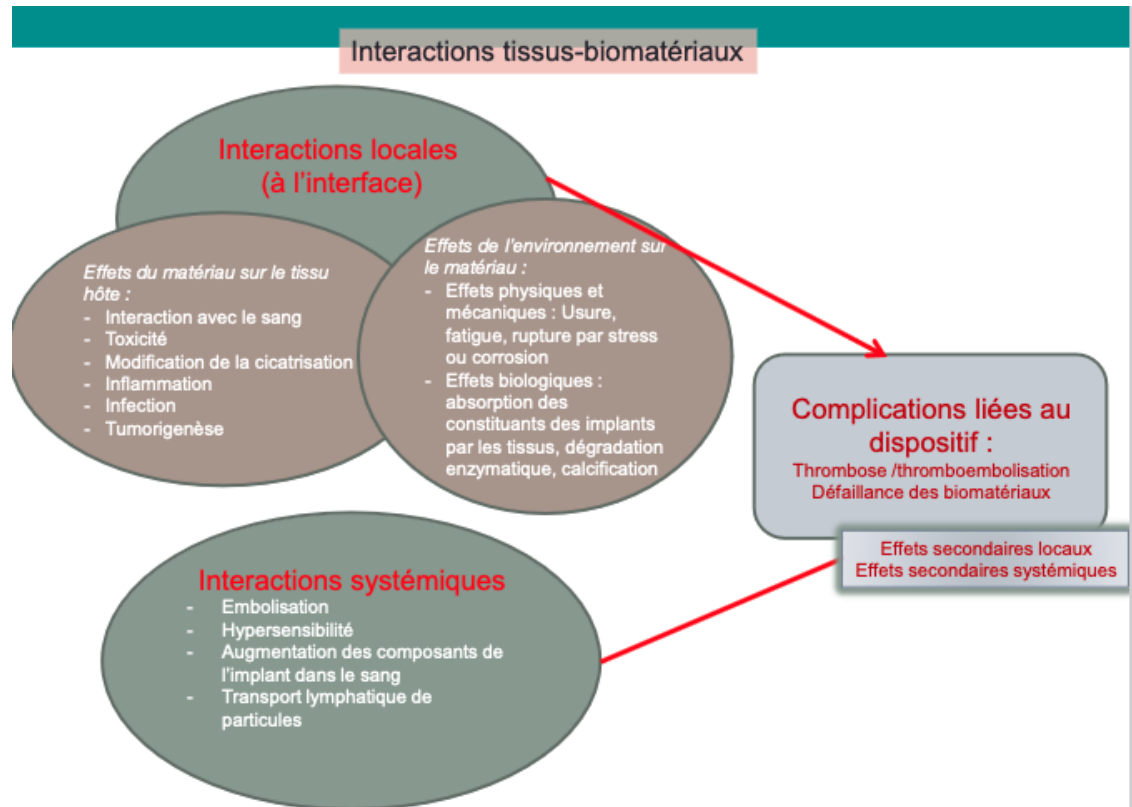
- Microscopie à Force Atomique, AFM
 - IR – Réflexion Totale Atténuée, ATR-FTIR
 - X-Rays Photoelectron Spectroscopy, XPS
 - Microscopie Electronique à Balayage, MEB
 - Mouillabilité, mesure des angles de contact
- Jean-Philippe Michel
- Caroline Aymes-Chodur



Matériaux Synthétiques

Matériaux Biosourcés

Caractérisation physico-chimique





Matériaux Synthétiques

Matériaux Biosourcés

Caractérisation physico-chimique

Charge de surface

Chimie de surface

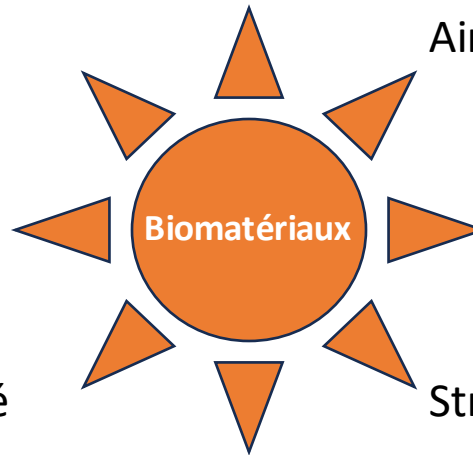
Aire de la surface

- FTIR-ATR,
- XPS,
- MEB

- MEB,
- AFM, STM

- Mouillabilité

Hydrophilicité
Hydrophobicité



Forme, topographie

Porosité

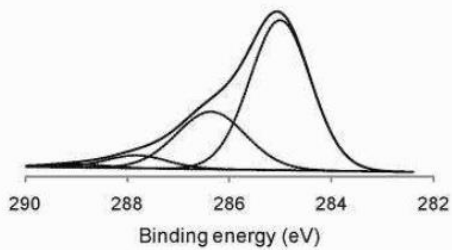
Structure cristalline

- MEB,
- AFM, STM

Défauts

Caractérisation physico-chimique

X-Rays Photoelectron Spectroscopy

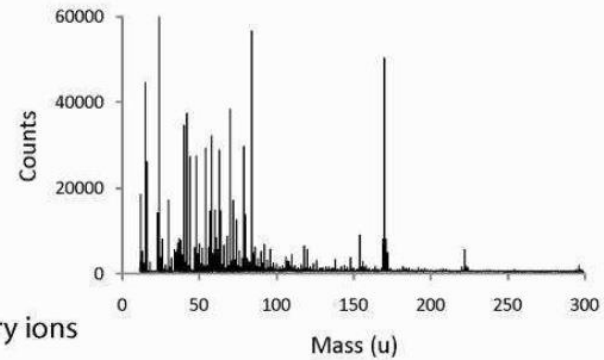
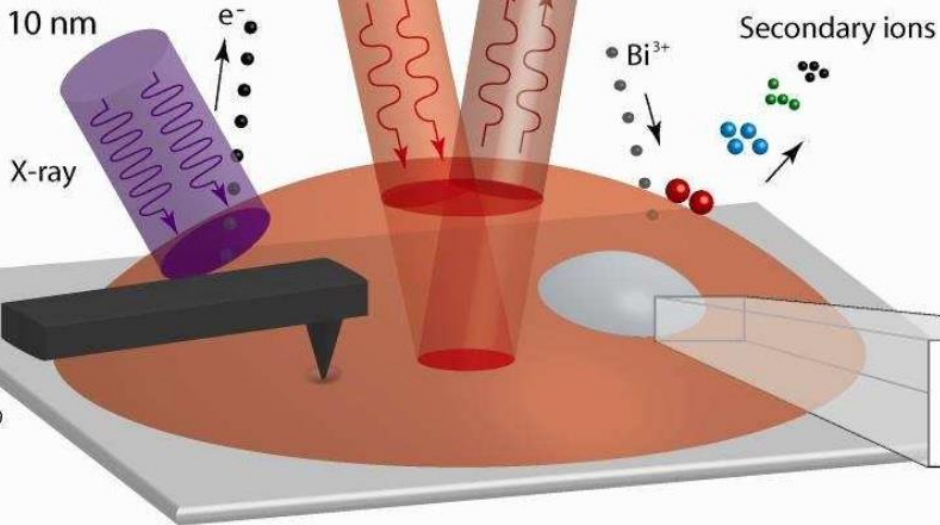


- XPS**
- Elemental and chemical composition
 - Sample top 10 nm

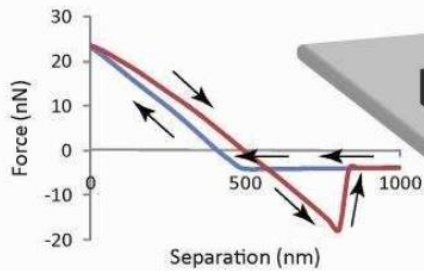
IR-ATR

- Raman or IR microspectroscopy
- Chemical functionality
 - Sample entire sample

Incident light Reflected light

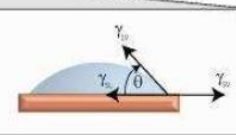


- ToF-SIMS**
- Chemical functionality
 - Sample top 2 nm



- Force measurements**
- Elastic modulus
 - Hardness
 - Roughness

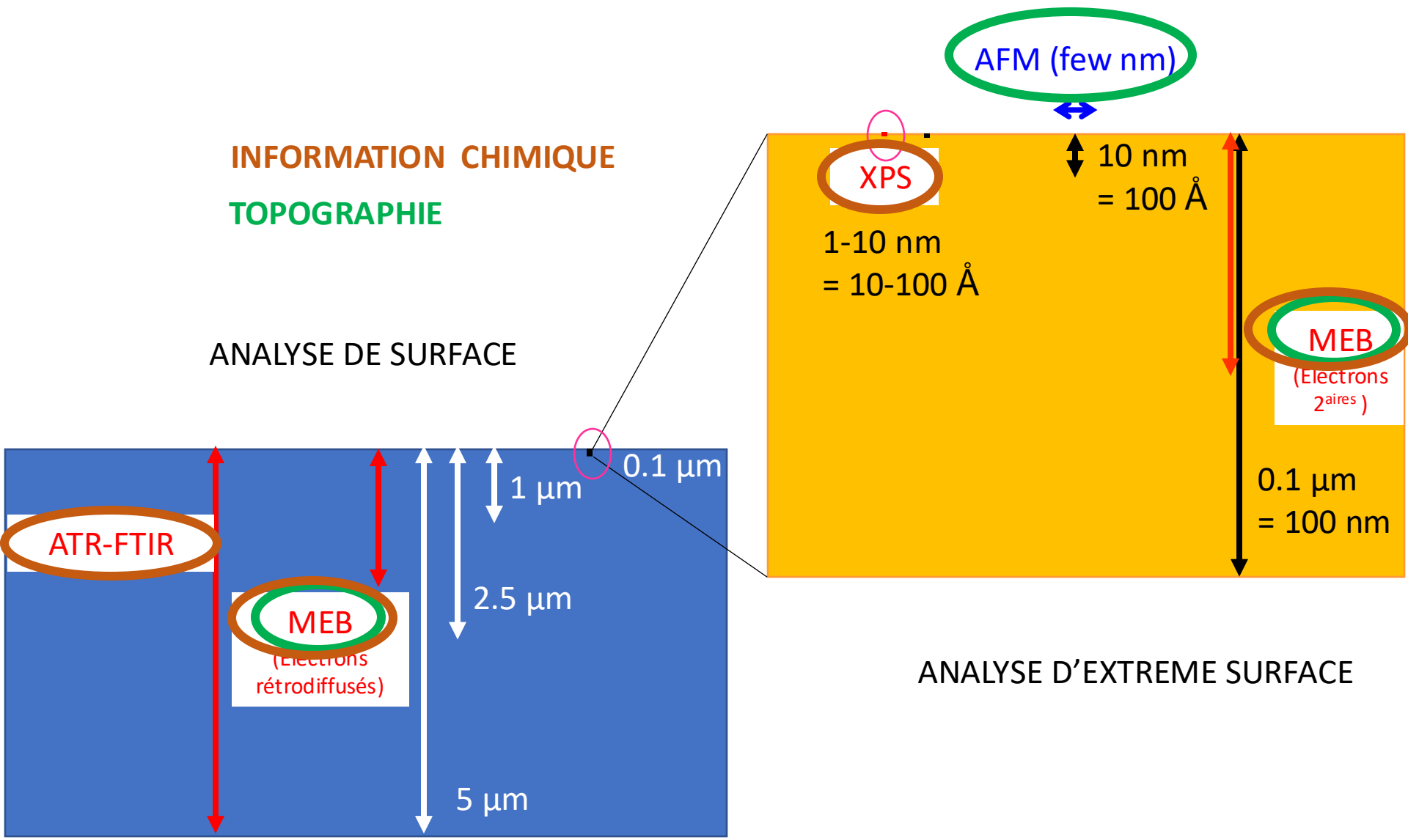
AFM

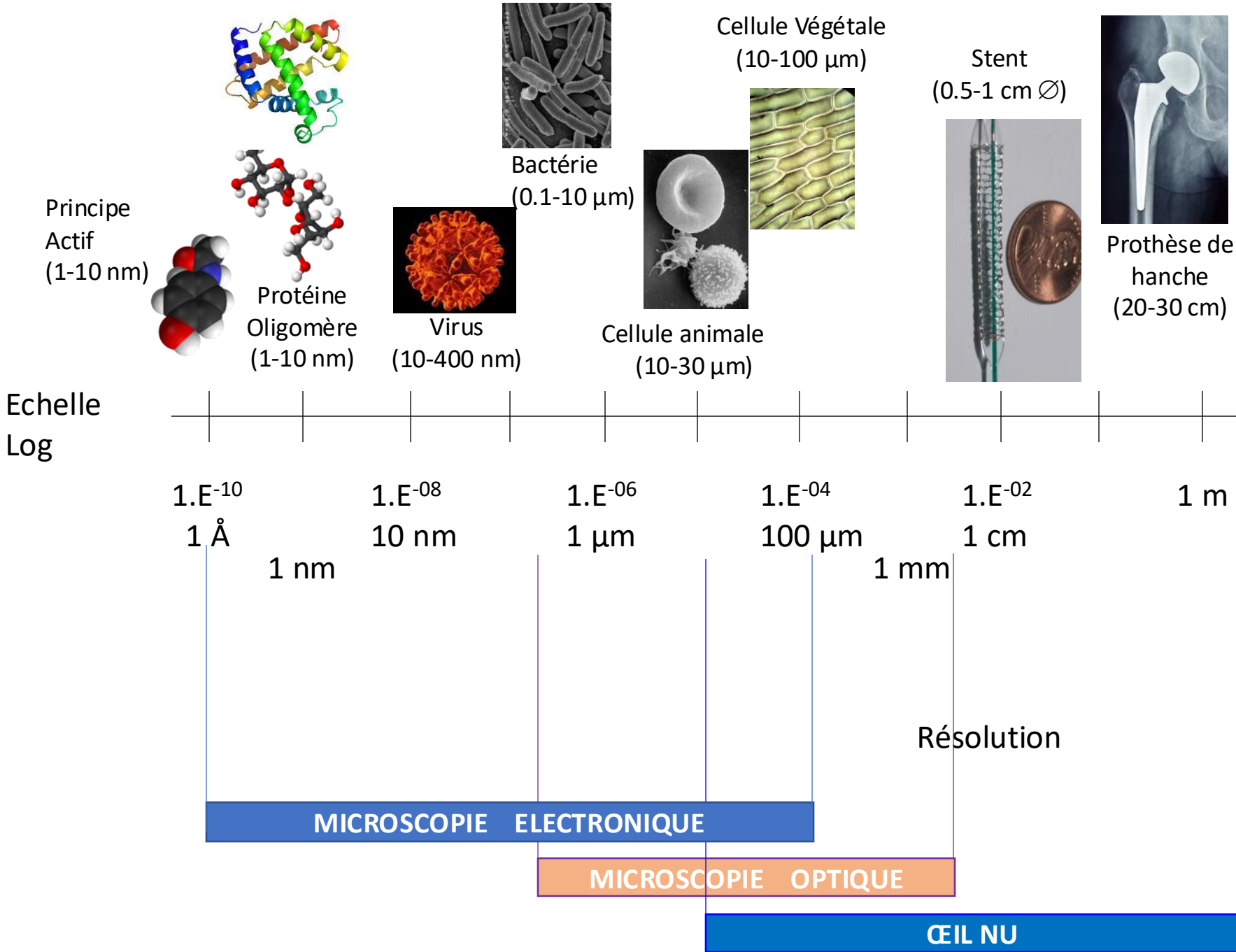


- WCA**
- Wettability
 - Sample top 1 nm

Mouillabilité

Selon les techniques, différentes informations sont obtenues :





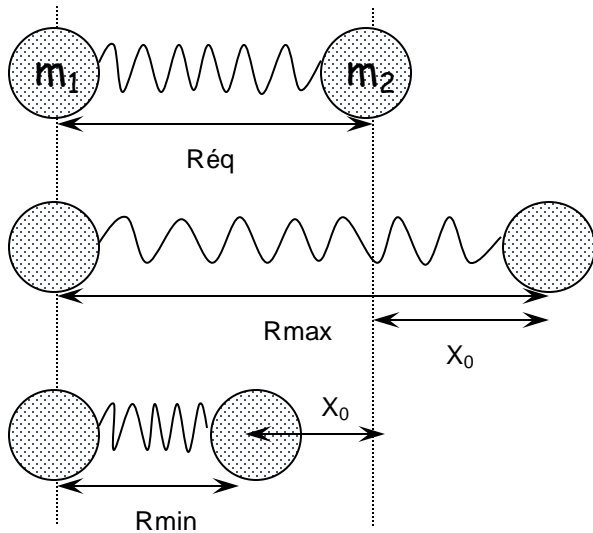
Analyse de Surface

- IR – Réflexion Totale Atténuée, ATR-FTIR
- X-Rays Photoelectron Spectroscopy, XPS
- Microscopie Electronique à Balayage, MEB
- Mouillabilité, mesure des angles de contact

Réflexion Totale Atténuée – Spectroscopie IR

ATR - FTIR

FTIR : modèle théorique de l' **oscillateur harmonique** \Rightarrow **INTERACTIONS VIBRATIONNELLES**



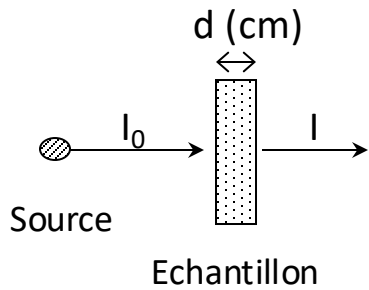
Energie vibrationnelle (E_{vib})

$$E_{vib} = \frac{1}{2} k X_0^2$$

Avec k , le tenseur du ressort (rigidité)

Liaison chimique = Ressort

2 modes majoritaires en FTIR: **transmission** / **réflexion**

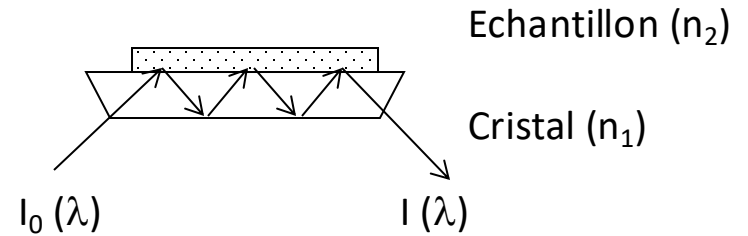


(C en mol.L⁻¹ et \mathcal{E} en L.mol⁻¹.cm⁻¹)

Mode TRANSMISSION



Toute l'épaisseur de l'échantillon est analysée



Mode REFLEXION

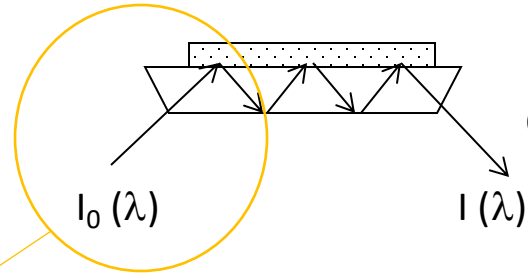


Seulement **quelques micromètres** (4-10 μm) de l'échantillon sont analysés



Seulement la surface

Mode REFLEXION : Attenuated Total Reflexion (ATR-FTIR)



Echantillon (n_2)

Cristal (n_1): ZnSe, Ge, C diamant

$I_0(\lambda)$

$I(\lambda)$

Onde évanescente

dp : Profondeur de pénétration (μm)

n_2

n_1

θ

Faisceau rétrodiffusé

$I_0(\lambda)$

$I(\lambda)$

Faisceau Incident

Faisceau Réfléchi

$$dp = \frac{\lambda}{2 \cdot \pi \cdot n_1 \cdot (\sin^2 \theta - (n_2/n_1)^2)^{1/2}}$$

Ex : $\left\{ \begin{array}{l} \text{PS } (n_2 = 1,59) \text{ sur ZnSe } (n_1 = 2,42) \\ \theta = 45^\circ \end{array} \right.$

Conditions pour la réflexion totale

$$\sin \theta \geq \frac{n_2}{n_1}$$

n_1 (prisme) > n_2 (échantillon)

\Rightarrow @ 2925 cm^{-1} , $dp = 1,1 \mu\text{m}$

\Rightarrow @ 796 cm^{-1} , $dp = 3,2 \mu\text{m}$

RESEARCH ARTICLE

Surface characterization of poly(lactic acid)/everolimus and poly(ethylene vinyl alcohol)/everolimus stents

Substance active utilisée pour prévenir d'un rejet cellulaire

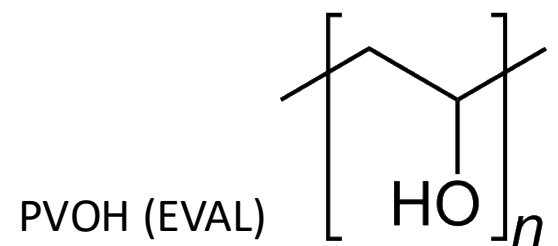
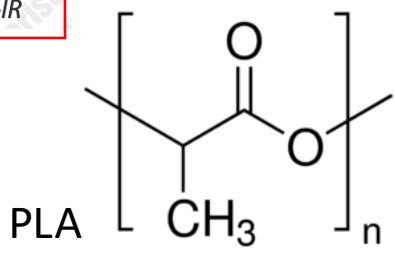
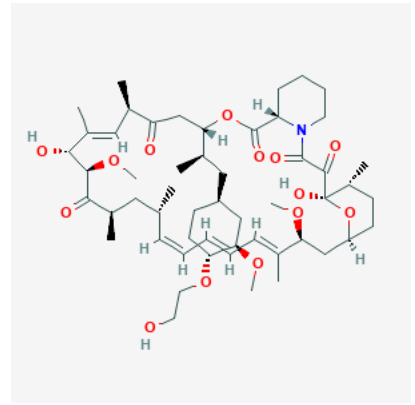
Ming Wu¹, Lothar Kleiner², Fuh-Wei Tang², Syed Hossainy², Martyn C. Davies¹, and Clive J. Roberts¹

¹Laboratory of Biophysics and Surface Analysis, School of Pharmacy, The University of Nottingham, NG7 2RD, UK, and ²Abbott Vascular, CA, USA

Abstract

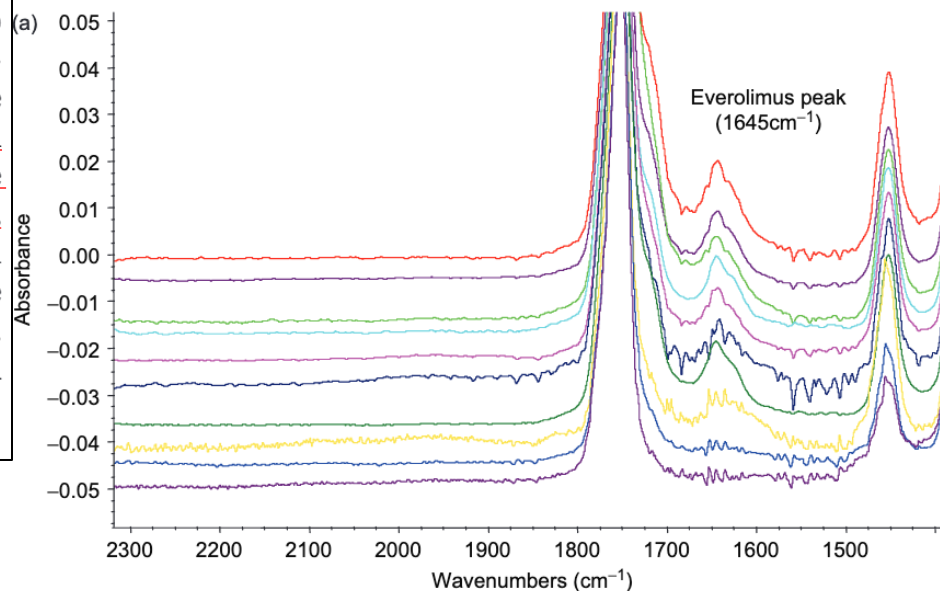
Two model drug eluting stents of poly(lactic acid) (PLA)/everolimus and poly(ethylene vinyl alcohol) copolymer (EVAL)/everolimus have been investigated using complementary surface analysis techniques including AFM, XPS, and ATR-IR to assess their structure and its relation to drug release. Different surface morphologies were observed for these stents, with phase separation evident on the PLA coating and a homogeneous system for the EVAL-based coating. This indicates a potentially different drug distribution for the different stents, although both showed a surface enrichment of the drug compared to the bulk. Dissolution studies for PLA/everolimus stents showed an immediate loss of drug from the surface as well as a longer term polymer matrix erosion. The EVAL/everolimus stent also displayed a loss of drug from its surface, but an intact surface after 28 days in dissolution media. These data are discussed in relation to the different release mechanisms occurring in the stents.

Keywords: Drug eluting stent; everolimus; AFM; XPS; ATR-IR

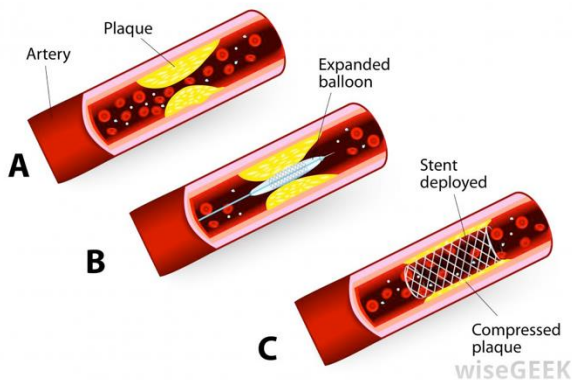


Attenuated total internal reflection infra-red spectroscopy (ATR-IR)

An Avatar 360 Inspect IR spectrometer equipped with silicon crystal was employed (Thermo Nicolet, Waltham, MA). The stents samples were pressed into intimate optical contact before and after dissolution with the top surface of the ATR silicon crystal for analysis in the infra-red range of $4000\text{--}500\text{ cm}^{-1}$ with 256 times scans at the resolution of 1 cm^{-1} for each position. ATR-IR was applied to identify the chemical information of the near surface region to $\sim 1\text{ }\mu\text{m}$ in depth to investigate drug distribution. Characterization was performed on the drug powder and polymer only coated stents first to obtain the reference IR spectra before the analysis of the drug-loaded stents. Representative peaks for everolimus were at 1645 cm^{-1} and 990 cm^{-1} , for PLA at 1268 cm^{-1} , and for EVAL at 835 cm^{-1} .



ANGIOPLASTY



Stent actif (libération contrôlée de l'everolimus)

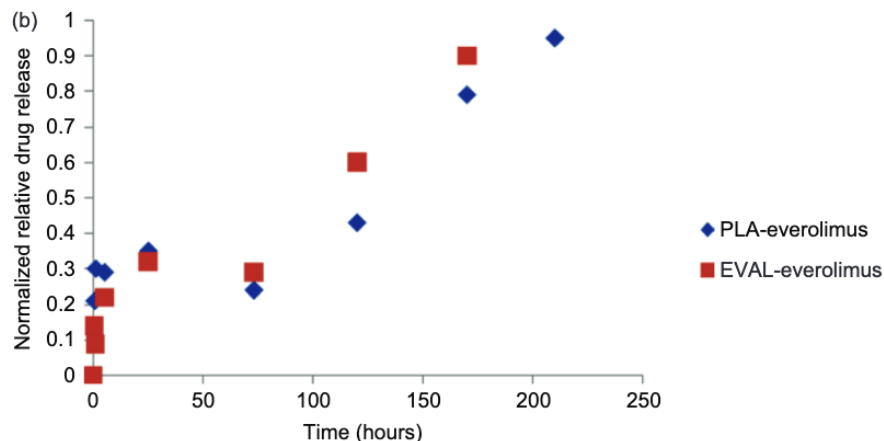


Figure 4. (a) ATR-IR spectra of dissolved PLA/everolimus coated stents (50wt%/50wt drug polymer ratio) at different time points (from top to bottom) of 0, 0.5, 1, 2, 6, 24, 72, 120, 168, and 216 h. The peak at 1645 cm^{-1} was contributed from everolimus only. (b) Near surface drug release profiles of PLA/everolimus and EVAL/everolimus-coated stents (50wt%/50wt drug polymer ratio) derived from ATR-IR spectra at the release in 1% Triton XL-80N up to 216 h.

Mise en évidence d'une nette diminution de l'intensité du pic représentatif du médicament à 1645 cm^{-1} au cours du temps.

Le rapport d'intensité du pic caractéristique du médicament (1645 cm^{-1}) sur celui du polymère (1268 cm^{-1}) permet de montrer la perte relative d'everolimus.

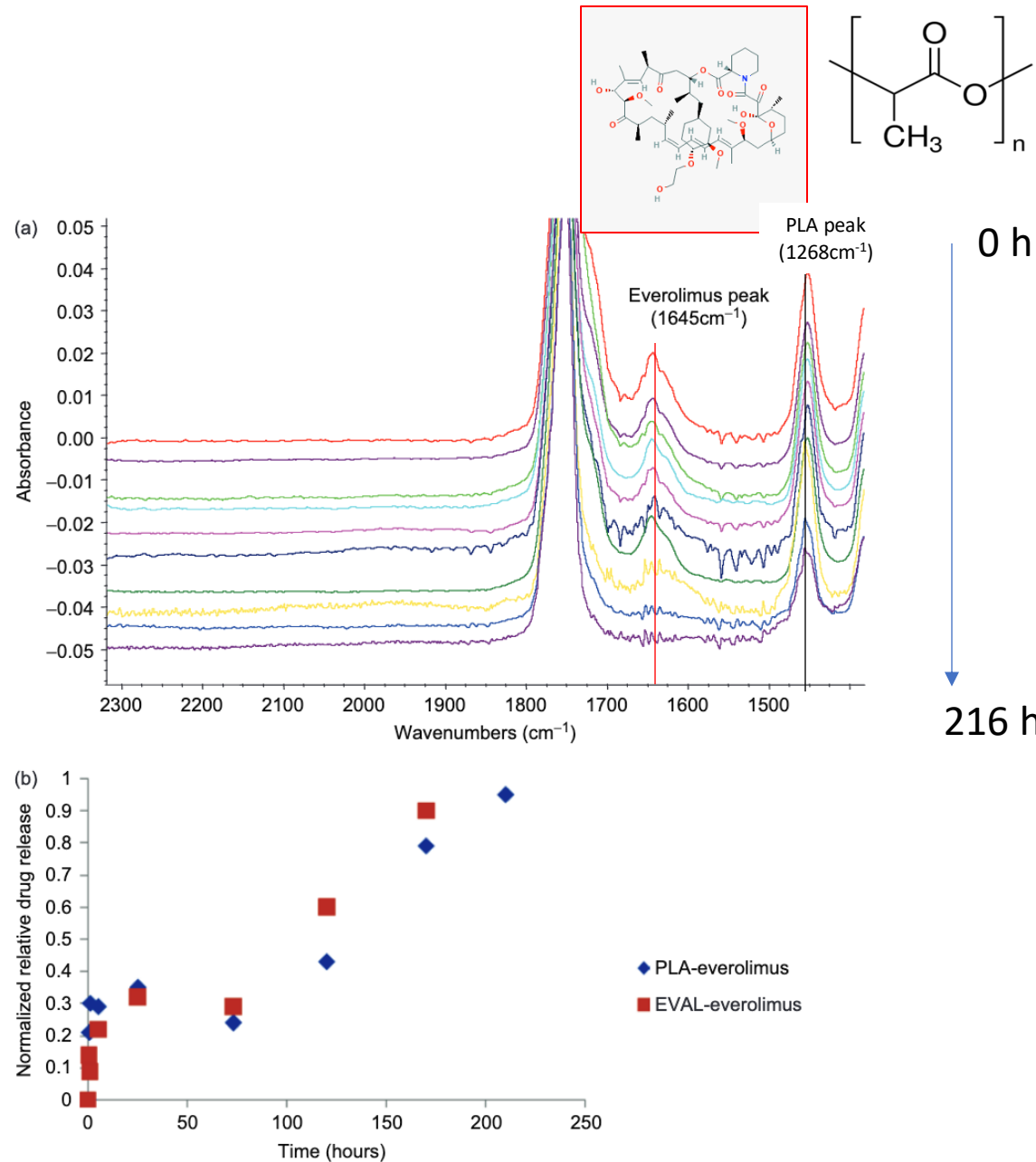


Figure 4. (a) ATR-IR spectra of dissolved PLA/everolimus coated stents (50wt%/50wt drug polymer ratio) at different time points (from top to bottom) of 0, 0.5, 1, 2, 6, 24, 72, 120, 168, and 216 h. The peak at 1645 cm^{-1} was contributed from everolimus only. (b) Near surface drug release profiles of PLA/everolimus and EVAL/everolimus-coated stents (50wt%/50wt drug polymer ratio) derived from ATR-IR spectra at the release in 1% Triton XL-80N up to 216 h.

Analyse de Surface

- IR – Réflexion Totale Atténuée, ATR-FTIR
- X-Rays Photoelectron Spectroscopy, XPS
- Microscopie Electronique à Balayage, MEB
- Mouillabilité, mesure des angles de contact

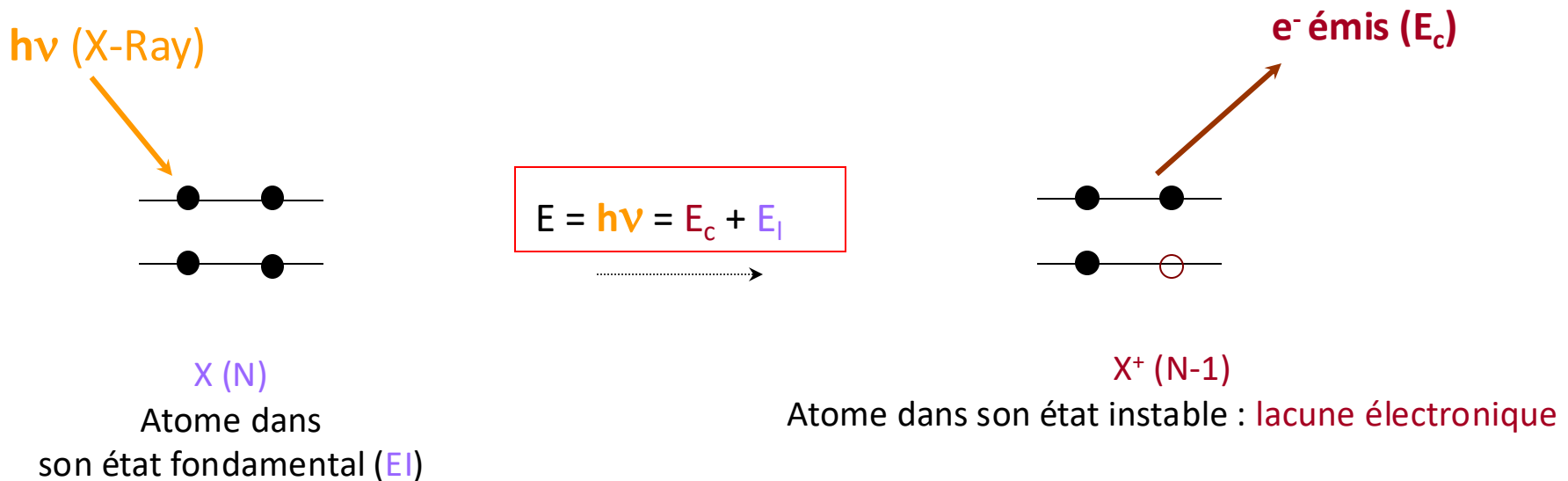
X-Rays Photoelectron Spectroscopy

XPS

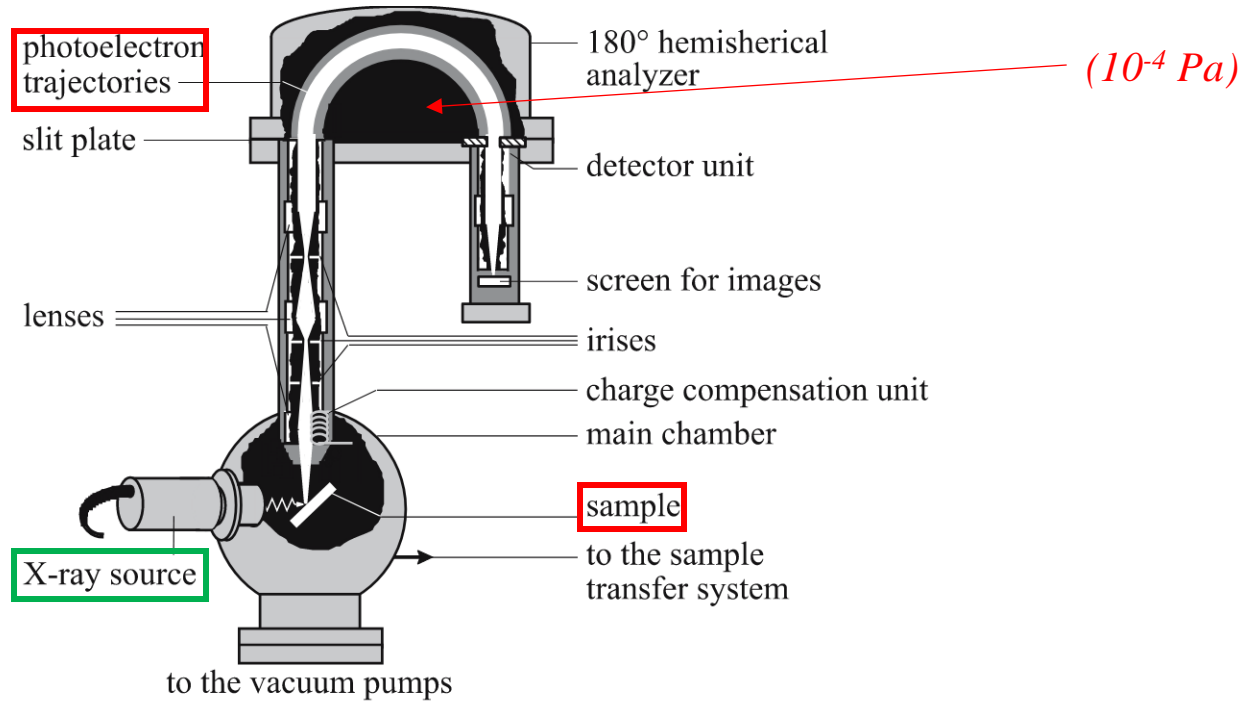
XPS (ou ESCA : Electron Spectroscopy for Chemical Analysis)

⇒ Technique d'analyse d'**extrême surface** (quelques 10 nm)

Repose sur l'**effet photoélectrique**

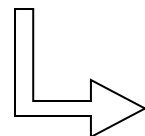


XPS Instrument :



Source de RX : Filament chauffé
(tube RX)

(ou R^t synchrotron
avec monochromateur)



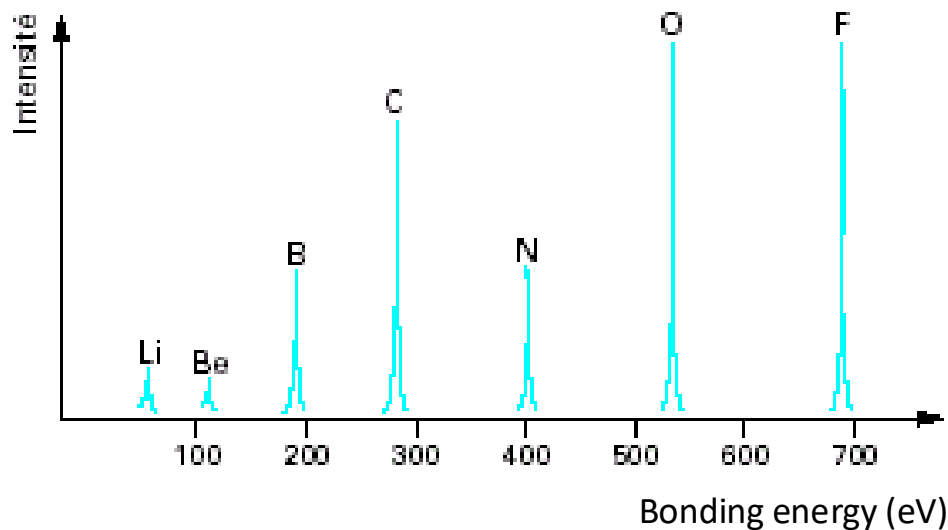
e^-

Anticathode

RX

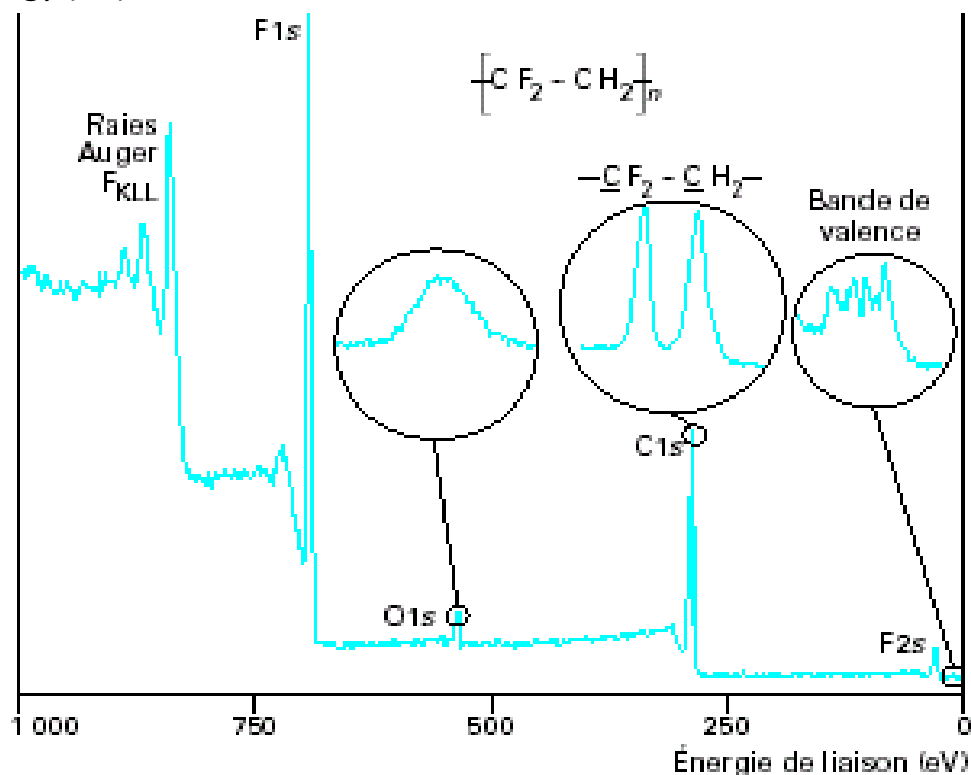
(Al : 1486,6 eV ou Mg : 1253,6 eV)

Pics 1s d'éléments de la 2^{ème} rangée du tableau périodique (Al K α = 1486,6 eV)



Z \nearrow , Energie de liaison \nearrow

Exemple du spectre de survol (survey)
du PVDF



RESEARCH ARTICLE

Surface characterization of poly(lactic acid)/everolimus and poly(ethylene vinyl alcohol)/everolimus stents

Ming Wu¹, Lothar Kleiner², Fuh-Wei Tang², Syed Hossainy², Martyn C. Davies¹, and Clive J. Roberts¹

¹*Laboratory of Biophysics and Surface Analysis, School of Pharmacy, The University of Nottingham, NG7 2RD, UK, and*

²*Abbott Vascular, CA, USA*

Abstract

Two model drug eluting stents of poly(lactic acid) (PLA)/everolimus and poly(ethylene vinyl alcohol) copolymer (EVAL)/everolimus have been investigated using complementary surface analysis techniques including AFM, XPS, and ATR-IR to assess their structure and its relation to drug release. Different surface morphologies were observed for these stents, with phase separation evident on the PLA coating and a homogeneous system for the EVAL-based coating. This indicates a potentially different drug distribution for the different stents, although both showed a surface enrichment of the drug compared to the bulk. Dissolution studies for PLA/everolimus stents showed an immediate loss of drug from the surface as well as a longer term polymer matrix erosion. The EVAL/everolimus stent also displayed a loss of drug from its surface, but an intact surface after 28 days in dissolution media. These data are discussed in relation to the different release mechanisms occurring in the stents.

Keywords: Drug eluting stent; everolimus; AFM; XPS; ATR-IR

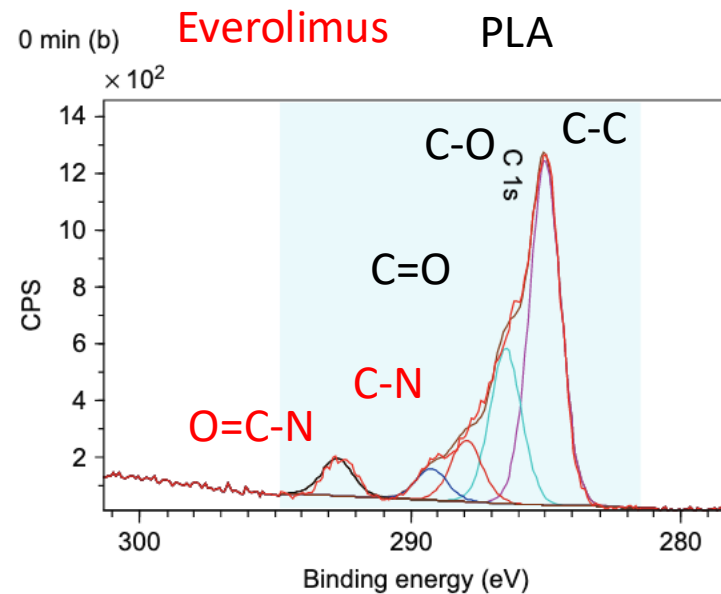
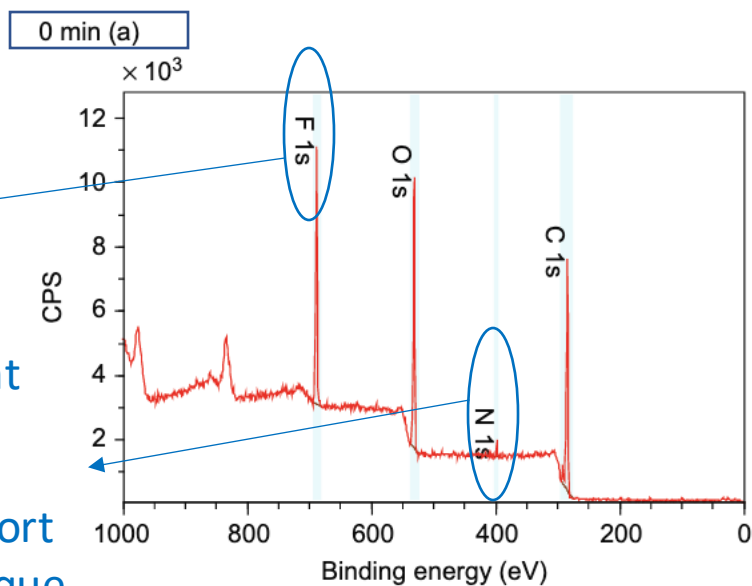
X-ray photoelectron spectroscopy (XPS)

The stent samples were scanned by X-ray photoelectron spectroscopy (Kratos AXIS ULTRA, Manchester, UK) with a monochromated Al K α X-ray source (1486.6 eV) operated at 15 mA emission current and 10 kV anode potential before and after dissolution. The take off angle for the photoelectron analyzer was 90°, with an acceptance angle of 30°. A magnetic immersion lens system allowed the area of analysis to be defined by apertures, a 'slot' aperture of 300 × 700 μm for wide/survey scans and high resolution scans.

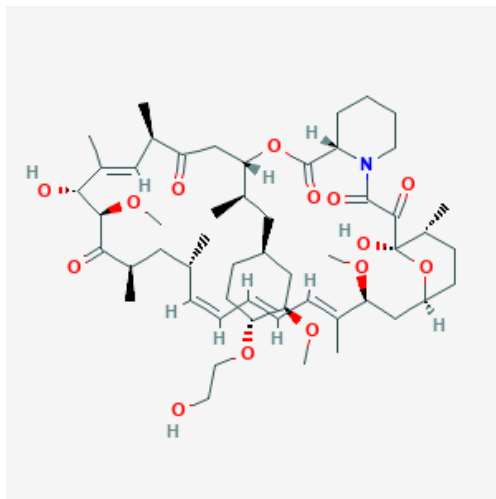
Avant dissolution

Contamination due au conditionnement du stent

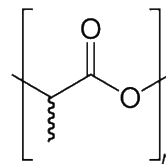
A partir du rapport N/C, on calcule que le %age de PA à la surface est ~ 85%



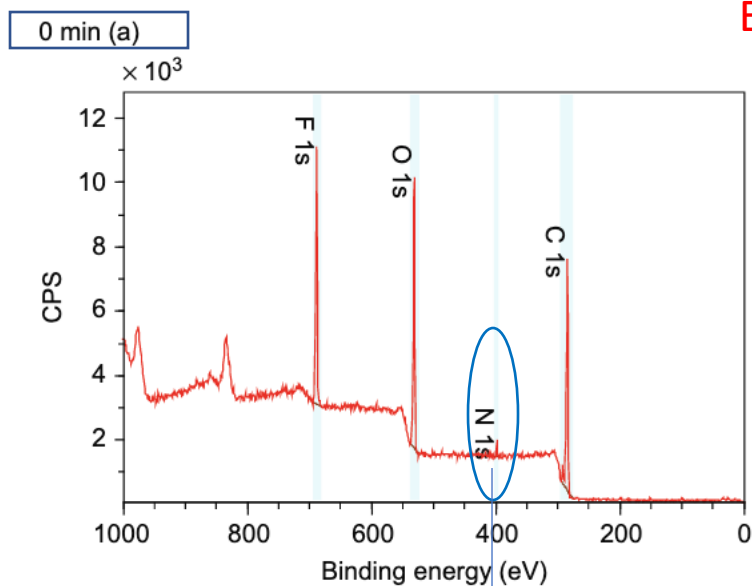
Everolimus: $C_{53}O_{14}NH_{83}$



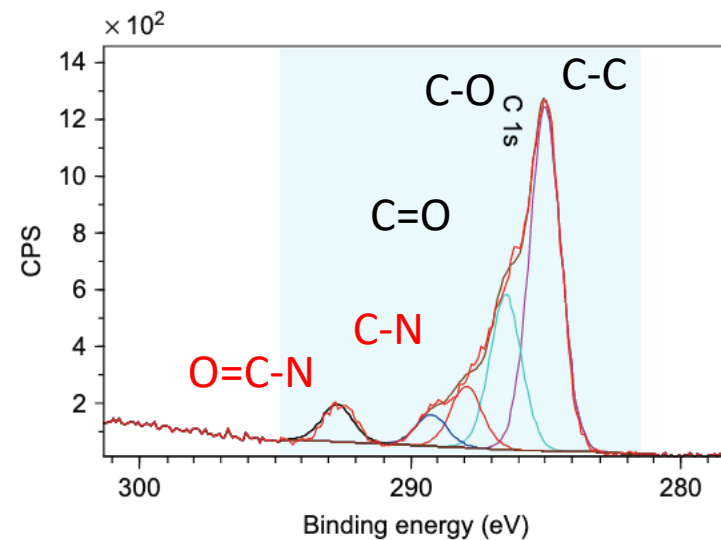
PLA



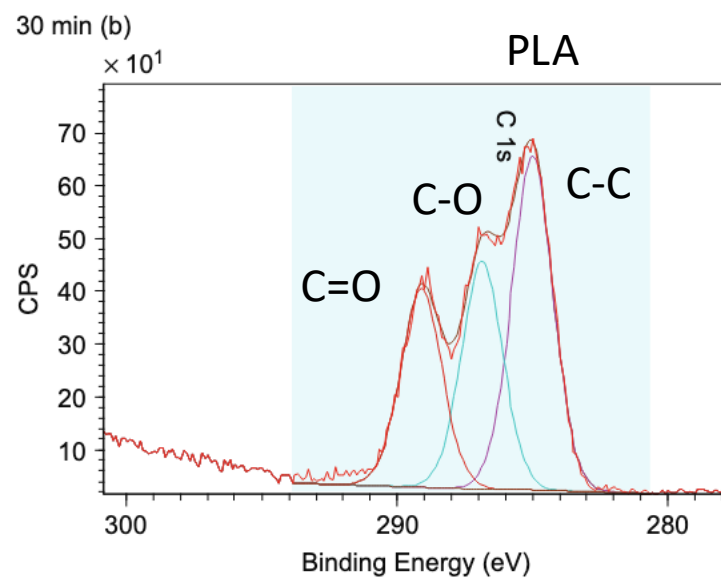
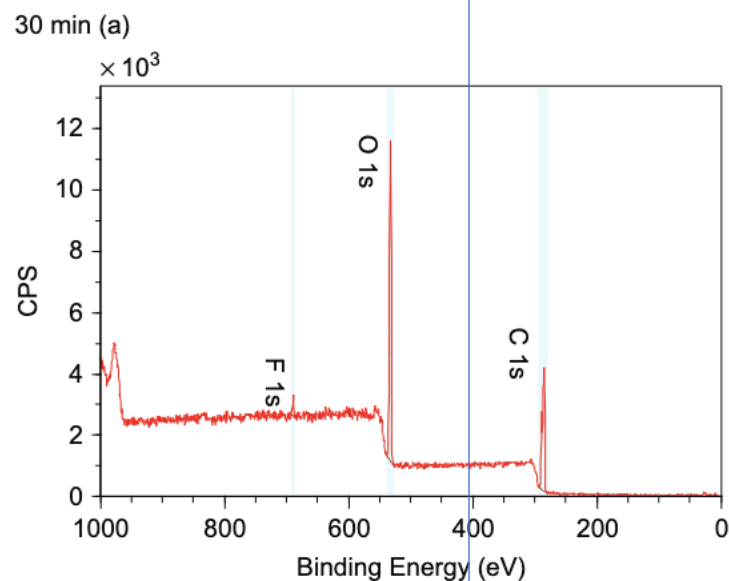
Avant
dissolution



Everolimus : $C_{53}O_{14}NH_{83}$ PLA



Après 30 min
dissolution



N_{1s} n'est plus détecté, ce qui signifie que le PA a été relargué au bout de 30 min \Rightarrow diffusion significative du PA (< 10 nm de profondeur pour l'analyse XPS).

Analyse de Surface

- IR – Réflexion Totale Atténuée, ATR-FTIR
- X-Rays Photoelectron Spectroscopy, XPS
- **Microscopie Electronique à Balayage, MEB**
- Mouillabilité, mesure des angles de contact

Microscope Electronique à Balayage

Technique d'analyse de surface pouvant être couplée à une analyse par EDS (Energy Dispersive Spectroscopy)

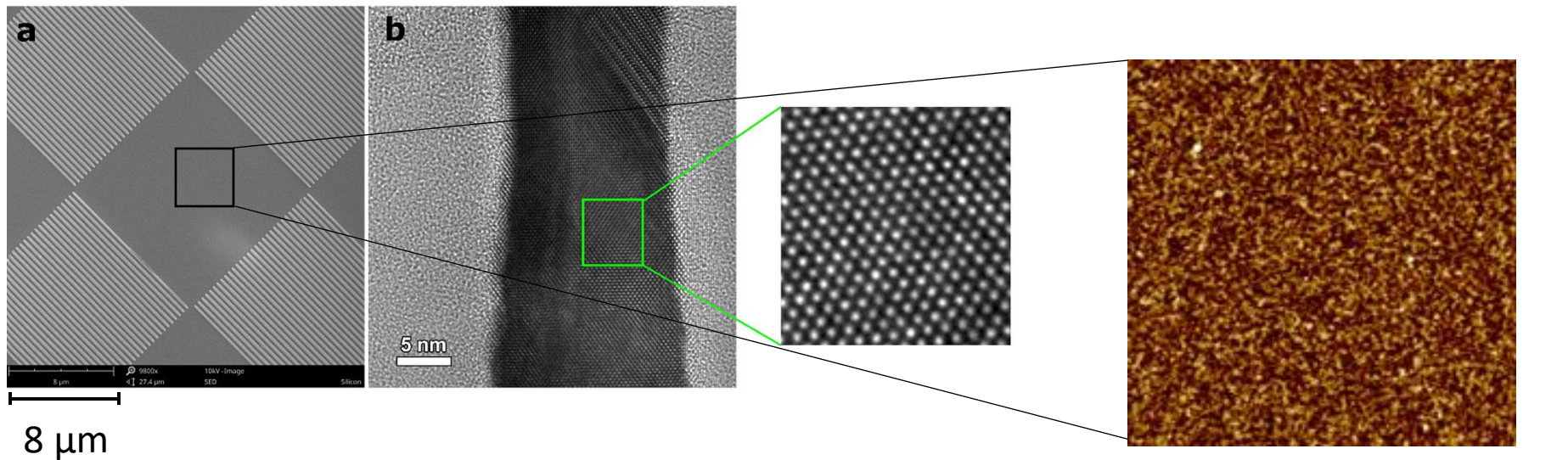
⇒ Répartition des atomes présents ($Z > 11$) en extrême surface (100 nm)

⇒ Technique **qualitative**.

Techniques de Microscopie :

- **SEM** : Scanning Electron Microscopy,
- **TEM** : Transmission Electron Microscopy,
- SPM : Scanning Probe Microscopy (**AFM** : Atomic Force Microscopy, STM : Scanning Tunneling Microscopy)

MEB, MET et AFM du silicium



MEB

**Morphologie,
composition**

MET

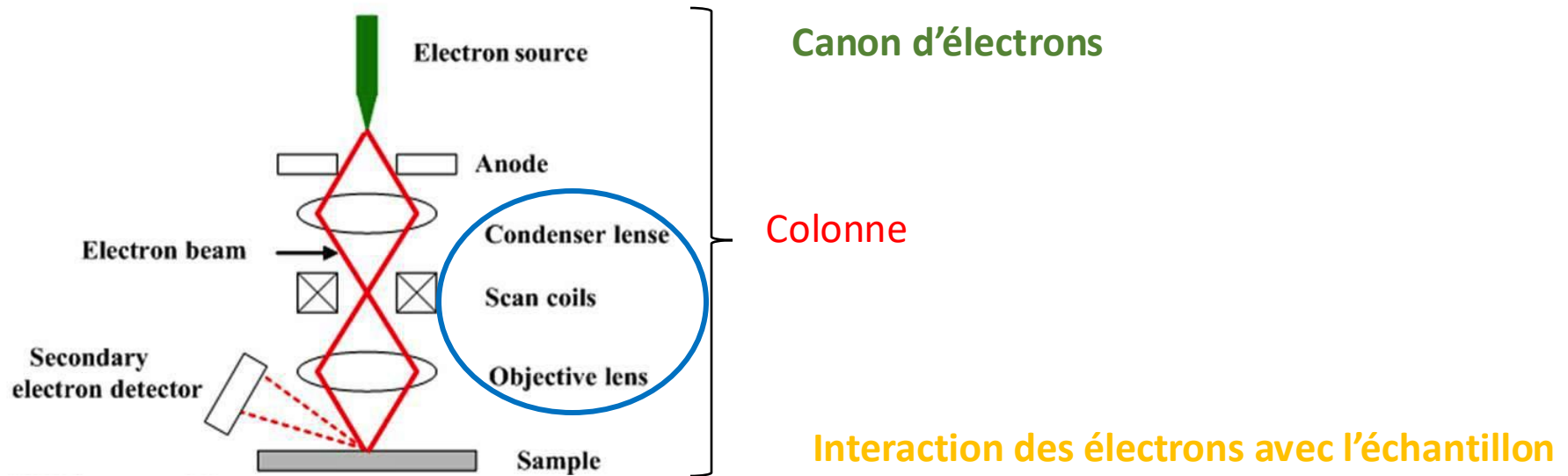
Information **structurelle** :
Les électrons traversent l'échantillon

AFM

Topographie de surface

Principe : différents composants du MEB

La microscopie électronique à Balayage (MEB) utilise **un faisceau focalisé d'électrons de haute énergie**.



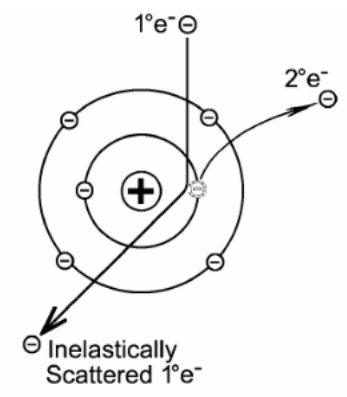
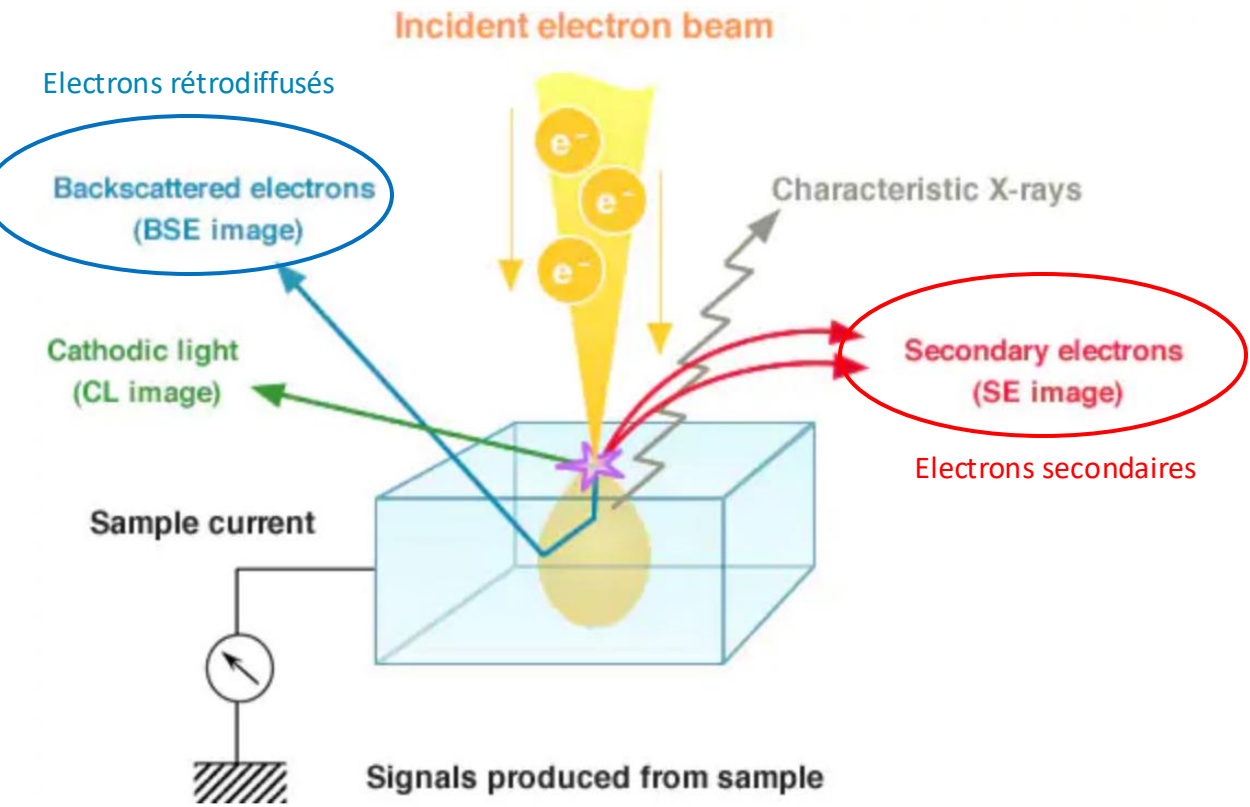
La colonne comprend 3 parties essentielles

Controlling the Path of Electrons

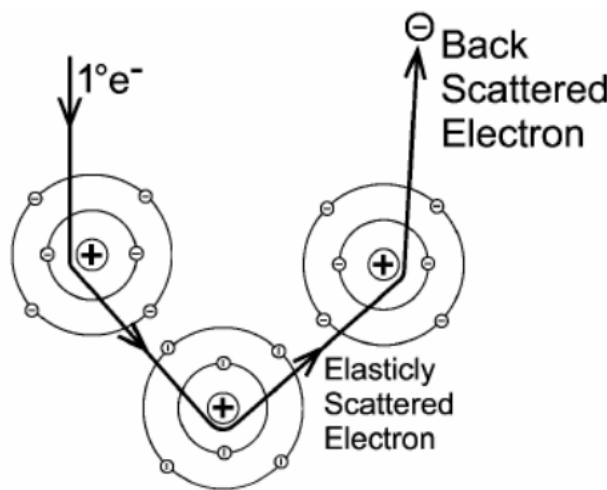
- **Lentilles Electromagnétiques** : définissent la taille du faisceau d'électrons (résolution)
- **Bobines de balayage** : alignent le faisceau sur l'échantillon
- **Lentilles Objectif** : focalisent le faisceau sur l'échantillon

Principe : différents composants du MEB

Interaction des électrons avec l'échantillon



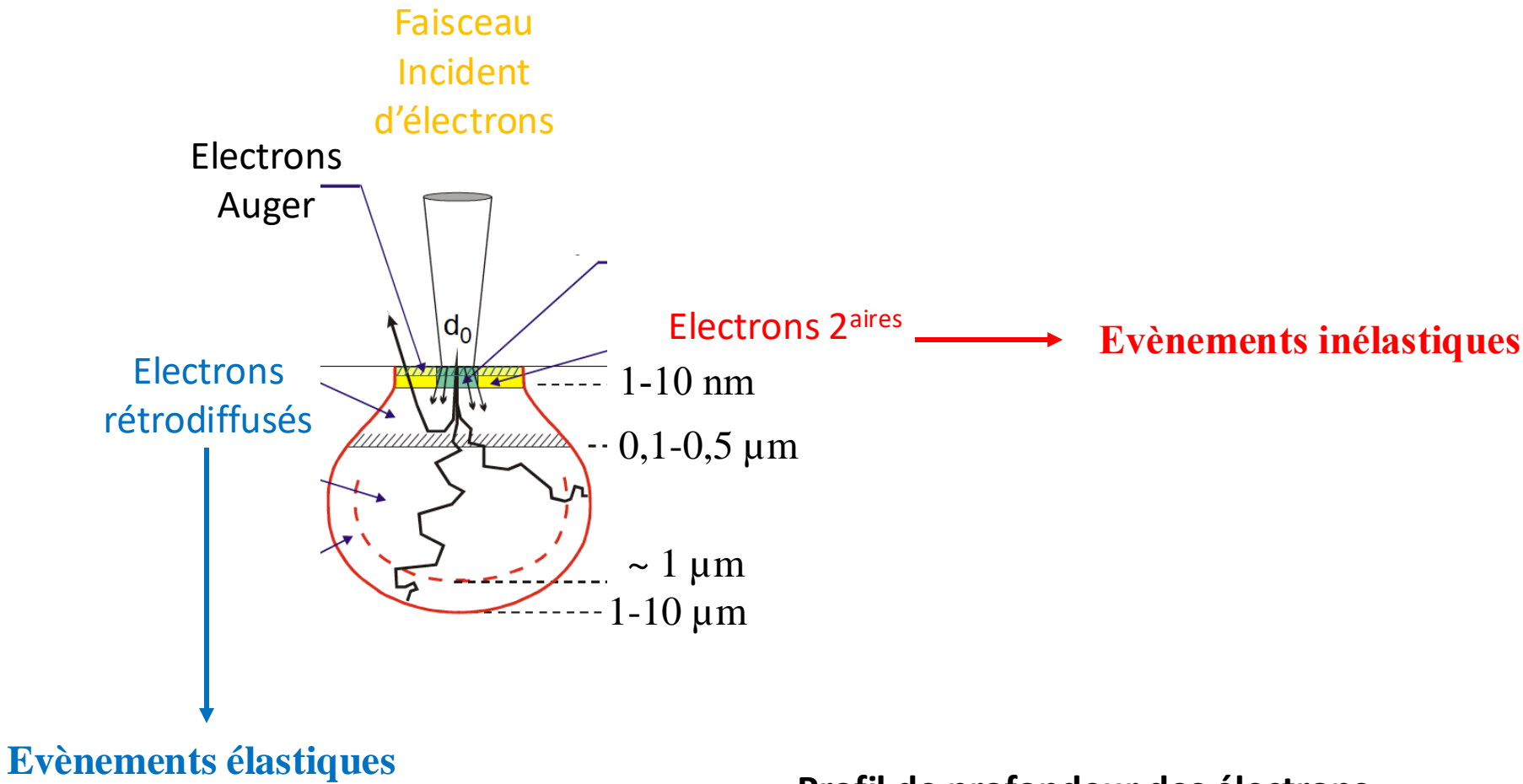
Evènements inélastiques



Evènements élastiques

Principe : différents composants du MEB

Interaction des électrons avec l'échantillon



Profil de profondeur des électrons
Volume d'interaction en forme de "poire"

Surface modification of endovascular stents with rosuvastatin and heparin-loaded biodegradable nanofibers by electrospinning

This article was published in the following Dove Press journal:
International Journal of Nanomedicine
29 August 2017
[Number of times this article has been viewed](#)

Milka Janjic^{1,2}
Foteini Pappa¹
Varvara Karagkiozaki¹
Christakis Gitas²
Kiriakos Ktenidis²
Stergios Logothetidis¹

¹Department of Physics, Laboratory for Thin Films – Nanosystems and Nanometrology, University of Thessaloniki, ²School of Medicine, Aristotle University of Thessaloniki, Thessaloniki, Greece

Abstract: This study describes the development of drug-loaded nanofibrous scaffolds as a nanocoating for endovascular stents for the local and sustained delivery of rosuvastatin (Ros) and heparin (Hep) to injured artery walls after endovascular procedures via the electrospinning process.

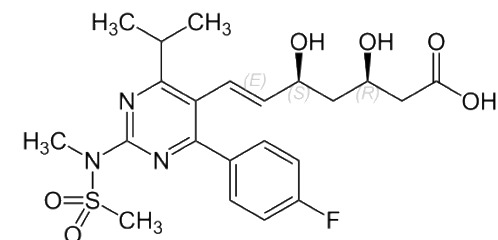
Purpose: The proposed hybrid covered stents can promote re-endothelialization; improve endothelial function; reduce inflammatory reaction; inhibit neointimal hyperplasia of the injured artery wall, due to well-known pleiotropic actions of Ros; and prevent adverse events such as in-stent restenosis (ISR) and stent thrombosis (ST), through the antithrombotic action of Hep.

Methods: Biodegradable nanofibers were prepared by dissolving cellulose acetate (AC) and Ros in *N,N*-dimethylacetamide (DMAc) and acetone-based solvents. The polymeric solution was electrospun (e-spun) into drug-loaded AC nanofibers onto three different commercially available stents (Co–Cr stent, Ni–Ti stent, and stainless steel stent), resulting in nonwoven matrices of submicron-sized fibers. Accordingly, Hep solution was further used for fibrous coating onto the engineered Ros-loaded stent. The functional encapsulation of Ros and Hep drugs into polymeric scaffolds further underwent physicochemical analysis. Morphological characterization took place via scanning electron microscopy (SEM) and atomic force microscopy (AFM) analyses, while scaffolds' wettability properties were obtained by contact angle (CA) measurements.

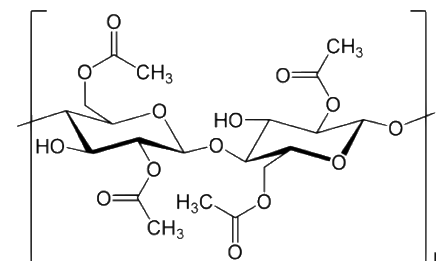
Results: The morphology of the drug-loaded AC nanofibers was smooth, with an average diameter of 200–800 nm, and after CA measurement, we concluded to the superhydrophobic nature of the engineered scaffolds. In vitro release rates of the pharmaceutical drugs were determined using a high-performance liquid chromatography assay, which showed that after the initial burst, drug release was controlled slowly by the degradation of the polymeric materials.

Conclusion: These results imply that AC nanofibers encapsulated with Ros and Hep drugs have great potential in the development of endovascular grafts with anti-thrombogenic properties that can accelerate the re-endothelialization, reduce the neointimal hyperplasia and inflammatory reaction, and improve the endothelial function.

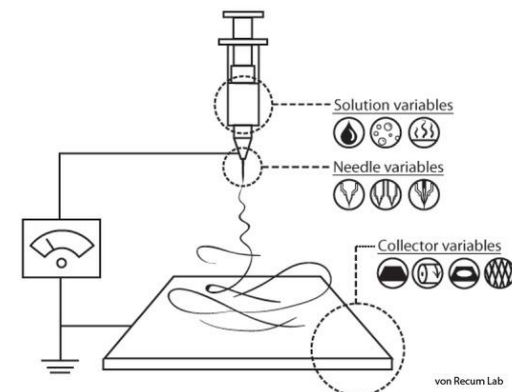
Keywords: cardiovascular disease, stent, drug delivery, scaffolds, nanocoating



Rosuvastatin (Ros)



Acétate de Cellulose



Electrospinning

Morphological evaluation by SEM

Information about the surface topography and composition of samples was obtained using SEM technique (JSM-6390LV; JEOL, USA). Samples were performed using standard stabilization protocol with glutaraldehyde and ethanol, with drying of the samples at the end. Drying of the samples was made in three cycles with the addition of aqueous solutions of ethanol concentration 70%, 90% and 100% v/v sequentially. Each solution was left at samples for ~30 min. After removing the last ethanol solution, samples were allowed to dry at room conditions in a laminar flow cabinet at air atmosphere. The diameter range of the fabricated nanofibers was measured via SEM images using the image visualization software ImageJ 1.34s (National Institutes of Health, AZ, USA). Average diameter and diameter distribution were determined by measuring 100 random nanofibers from the SEM images.

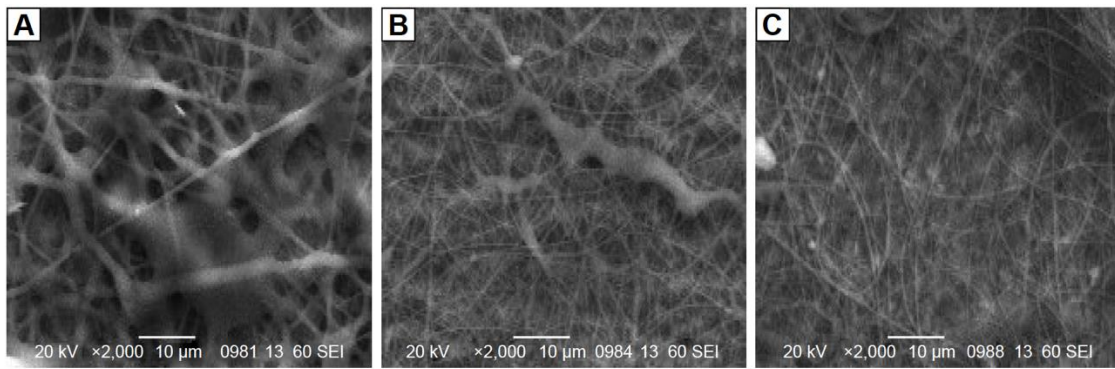
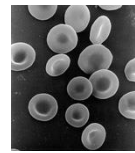


Figure 1 SEM images of (A) AC nanofibers, (B) AC nanofibers loaded with Ros, and (C) AC nanofibers loaded with Ros and Hep. **Note:** Scale bar: 10 µm. **Abbreviations:** SEM, scanning electron microscopy; AC, cellulose acetate; Ros, rosuvastatin; Hep, heparin.

Fibres sub-microniques en acétate de cellulose (200–800 nm de diameter) avec des diamètres de pores de 6 à 16 µm



La plus part des globules rouges ont des diamètres de l'ordre de 6–8 µm ⇒ Les pores du matelas de nanofibres non tissées sont **suffisamment larges pour laisser passer les globules rouges en microcirculation**, afin d'apporter un echnage suffisant en oxygène pour les tissus et organes.

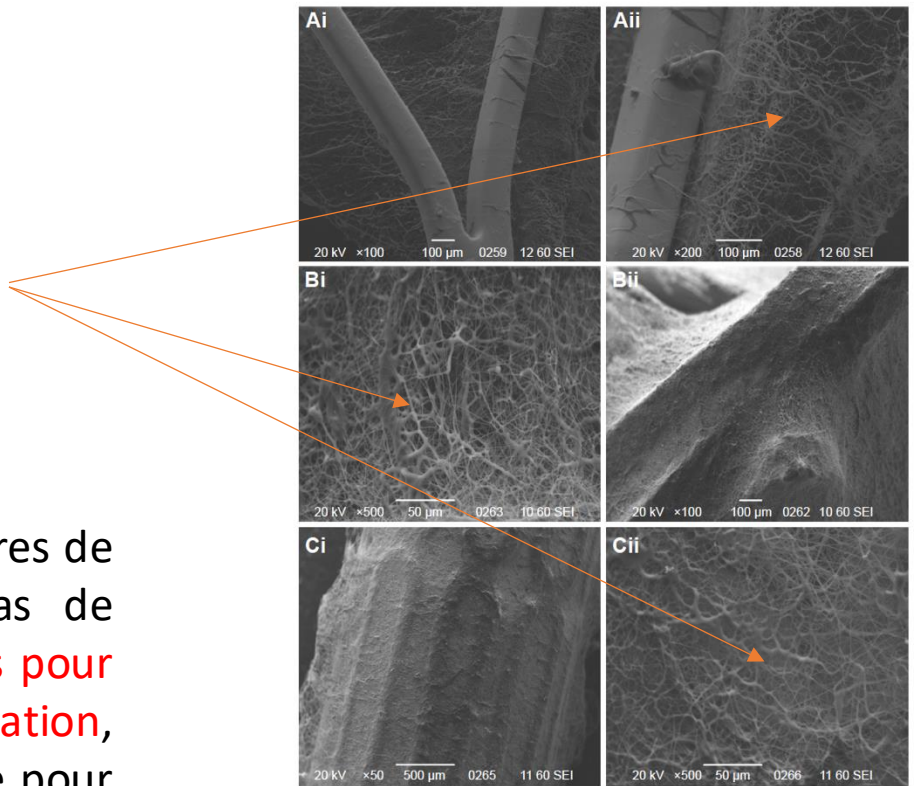


Figure 4 SEM images of (Ai) Ni-Ti stent with nanofibers, (Bi) stainless steel stent with nanofibers, and (Ci) Co-Cr stent with nanofibers. **Note:** (Aii–Cii) are magnified images of (Ai–Ci). **Abbreviations:** SEM, scanning electron microscopy; Ni-Ti, nickel-titanium alloy stent; Co-Cr, cobalt-chromium alloy stent.

Les résultats d'études de biodégradation in vitro ont montré que la dégradation des fibres non tissées biodégradables se faisait au bout de 60 jours.

14%
20%
AC drug loaded fibers

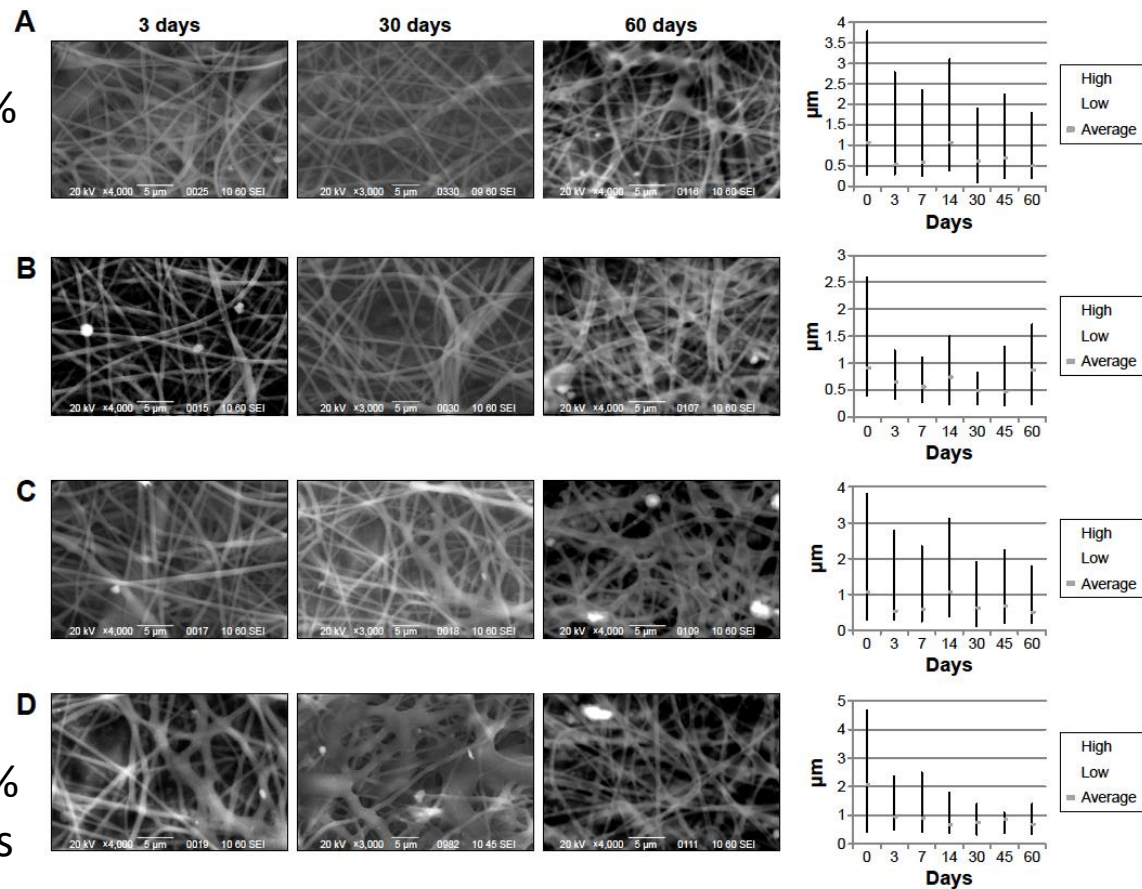


Figure 7 SEM images and diagrams of biodegradation of (A) 14%, (B) 16%, (C) 18%, and (D) 20% AC drug-loaded nanofibers at 3, 30, and 60 days. Note: 14%, 16%, 18%, and 20% are different concentrations of AC drug-loaded nanofibers. Abbreviations: SEM, scanning electron microscopy; AC, cellulose acetate.

- L'un des domaines de recherche en **nanomédecine** utilise des systèmes de libération contrôlée de pa (drug delivery systems) dans lesquels les nanofibres permettent **d'encapsuler** un agent thérapeutique.
- La cinétique pharmaceutique de libération de PA, dépend de la dégradation des fibres de polymère, qui peuvent être façonnées afin de contrôler le phénomène **d'encapsulation**.

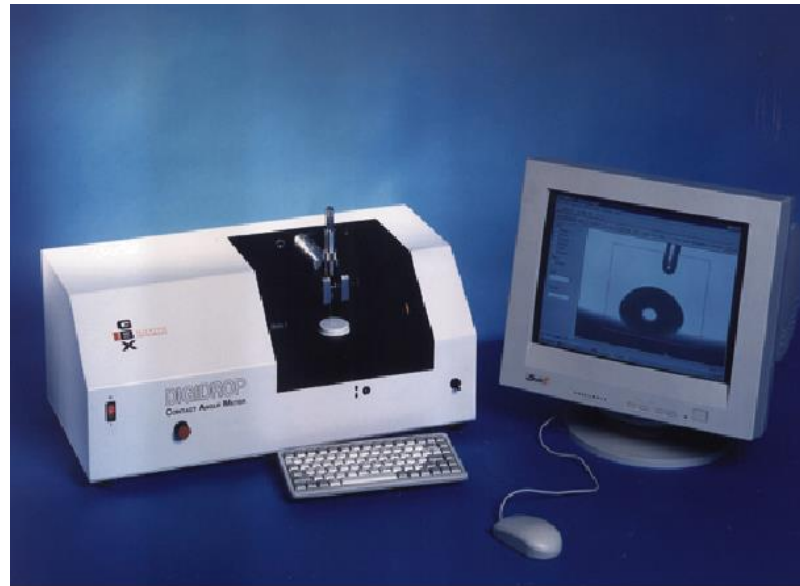
Analyse de Surface

- IR – Réflexion Totale Atténuée, ATR-FTIR
- X-Rays Photoelectron Spectroscopy, XPS
- Microscopie Electronique à Balayage, MEB
- **Mouillabilité, mesure des angles de contact**

MOUILLABILITE

Mouillabilité : Evaluer la capacité d'un substrat à être mouillé par un liquide

- ↪ Détermination de **l'angle de contact** solide/liquide
- ↪ Déterminer **l'énergie libre de surface** du solide
- ↪ Application à **différents types de traitements de surface**.

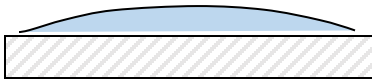


MOUILLABILITE

Mouillabilité : Evaluer la capacité d'un substrat à être mouillé par un liquide

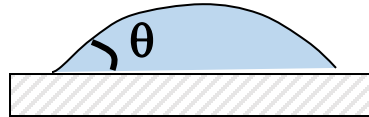
- ↪ Détermination de l'**angle de contact** solide/liquide
- ↪ Déterminer l'**énergie libre de surface** du solide
- ↪ Application à **différents types de traitements de surface**.

Cas où $\theta \sim 0$



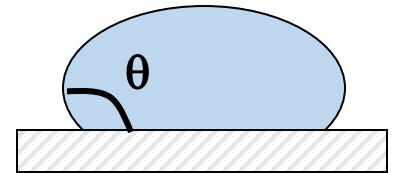
Surf. **parfait^t mouillable**

Cas où $\theta < 90^\circ$



Mouillage **imparfait**

Cas où $\theta > 90^\circ$

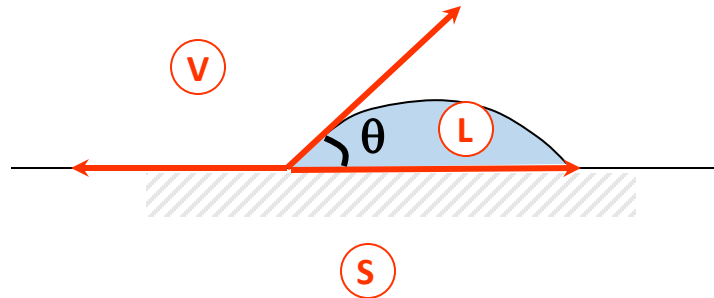


Pas de mouillage

Selon les propriétés hydrophile/hydrophobe entre le substrat et le liquide

⇒ Mesure de l'interaction : Applications en biologie, chimie des polymères, ...

MOUILLABILITE



L : Liquide,

S : Solide,

V : Vapeur,

θ : Angle de contact formé à la frontière entre 3 phases (solide, liquide, vapeur).

γ : Energie libre de surface (mN/m ou mJ/m²) : force qui s'exerce au point de contact entre les 3 phases.

Interface solide/liquide : correspond à un travail d'adhésion entre le liquide et le solide (w_{SL})

$$w_{SL} = \gamma_S + \gamma_L - \gamma_{SL}$$

γ_{SL} : tension **interfaciale** liquide/solide

γ_{LV} (γ_L) : tension superficielle du **liquide**

γ_{SV} (γ_S) : énergie de surface du **solide**

Cas des surfaces lisses

Relation d'**Young** :

$$\gamma_{SV} = \gamma_{SL} + \gamma_{LV} \cos\theta$$

→ Décrit l'**équilibre** entre les 3 phases

Mouillabilité

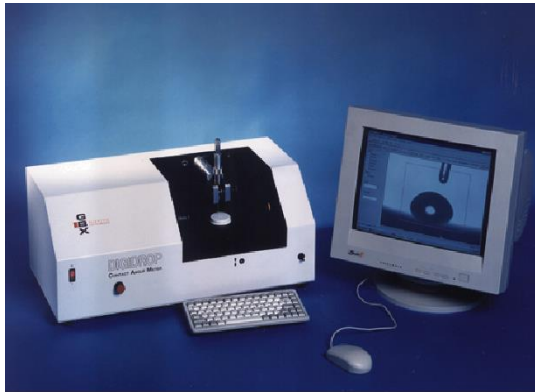
Mesure de l'angle de contact

Mesure de l'énergie de surface

θ : Angle de contact, mesuré à l'intérieur du liquide

⇒ Caractérise l'interaction solide/liquide

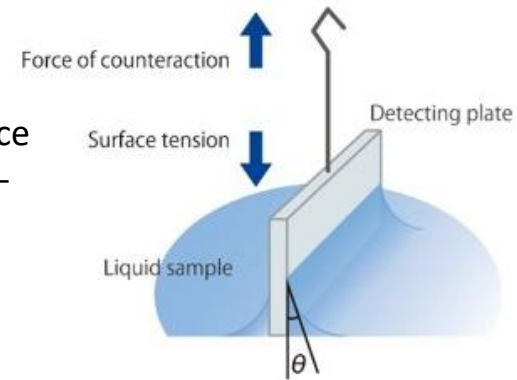
Détermination de la **tension superficielle** (2 méthodes : lame de Wilhemy / goutte pendante)



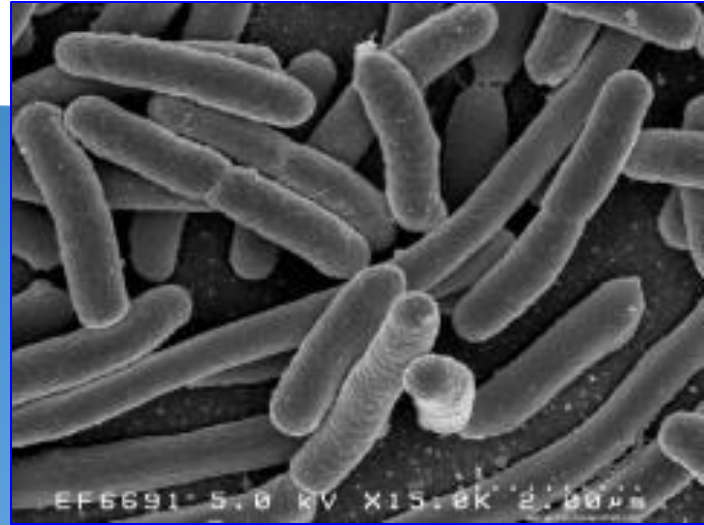
Tensiomètre de surface
(balance de Langmuir-Wilhelmy)

$$\gamma_L = \frac{F}{l}$$

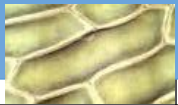
Avec l = périmètre de la plaque de platine



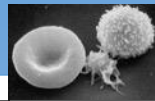
Bactérie 1-5 μm



Cellule Végétale
(10-100 μm)



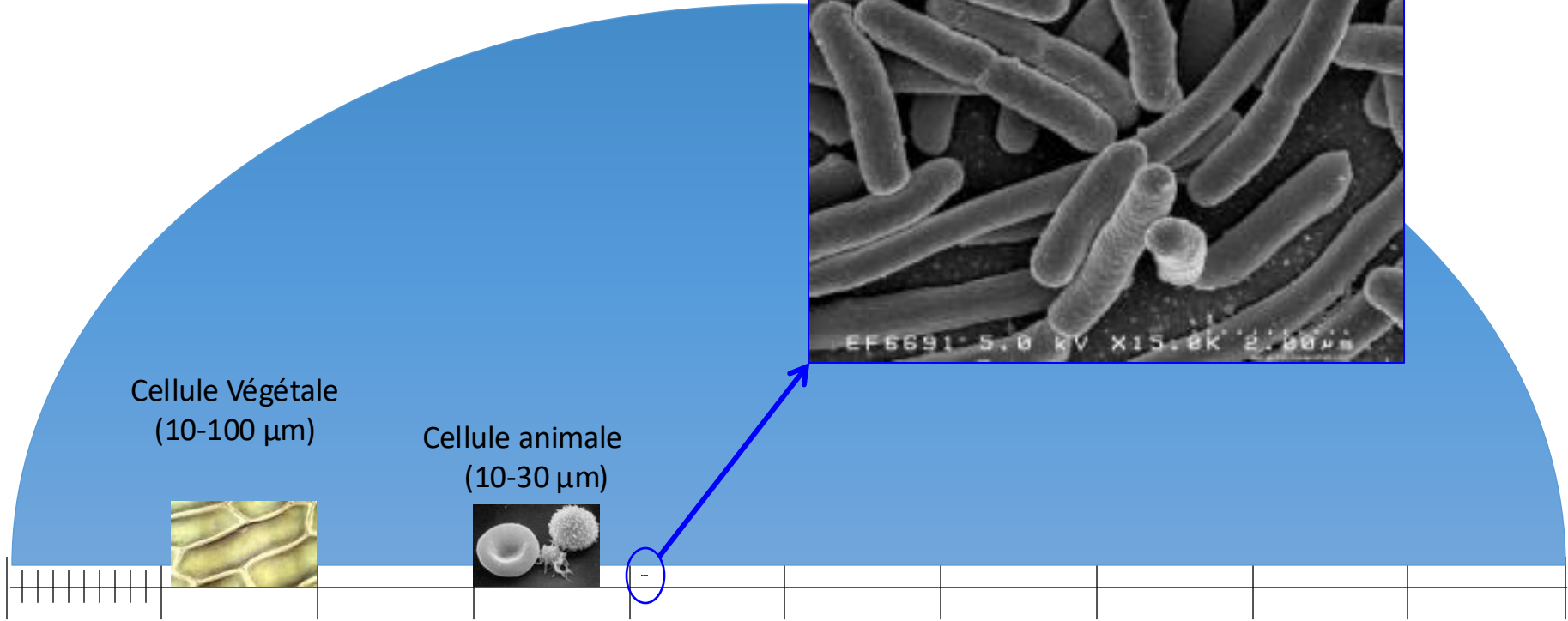
Cellule animale
(10-30 μm)



$1.E^{-04}\text{m} = 100 \mu\text{m}$

$1.E^{-05}\text{m} = 10 \mu\text{m}$

$1.E^{-03}\text{m} = 1 \text{ mm}$



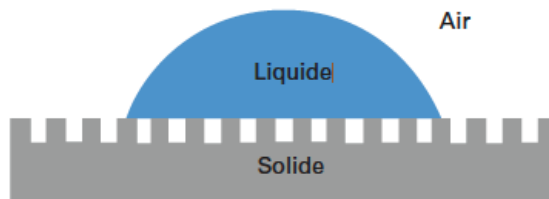
Mouillabilité des structures texturées

Lors que les surfaces ne sont pas lisses, la **texturation** de surface modifié le mouillage.

→ 4 régimes de mouillage : Cassie-Baxter, Wenzel, mixte et imprégné.

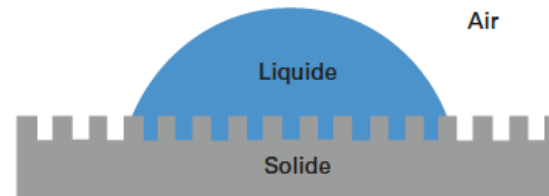
→ Cas des surfaces **super-oléophobes** ou **super-hydrophobes**.

Air piégé entre le liquide et le substrat



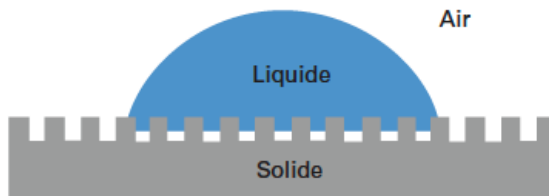
1- Régime Cassie-Baxter

Le liquide est en contact avec la surface texturée

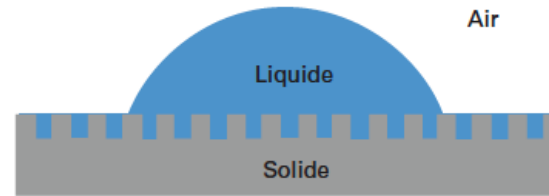


2- Régime Wenzel

Situation intermédiaire entre 1 et 2



3- Régime mixte



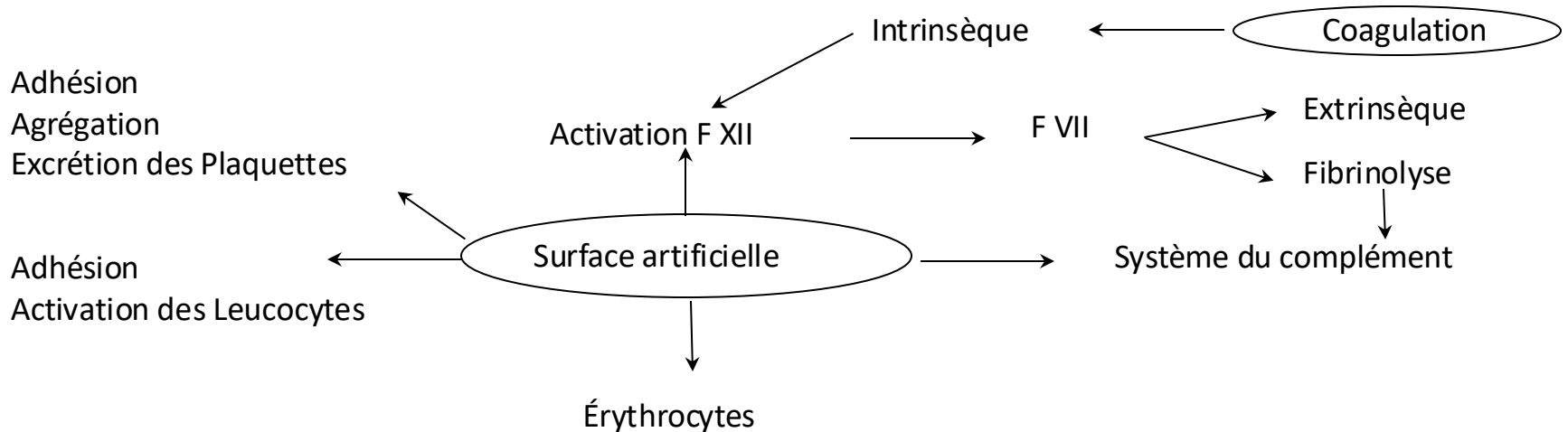
4- Régime imprégné

D'après *Techniques de l'ingénieur*, M1690, L. Vonna (2017); [10.1098/rsta.2010.0121](https://doi.org/10.1098/rsta.2010.0121), Bormashenko (2010)

CONCLUSIONS

Selon les propriétés physico-chimiques de surface, les réactions physiologiques avec les constituants sanguins sont influencées

↳ **Activation** de nombreuses réactions de défense de l'organisme en présence de ce matériau : **Phase de contact de la coagulation** (cf. Schéma).



↳ Mise en évidence par **mouillabilité** des propriétés physico-chimiques du matériau et prévision des interactions possibles avec le milieu biologique.

↳ Utilisation de la **MEB** pour décrire la morphologie de surface.

CONCLUSIONS

- Techniques d'analyse de surface afin d'étudier le matériau à travers différentes **profondeurs** et différentes **échelles**,
- Différentes informations : **rugosité, topographie, fonctions chimiques**
- Techniques complémentaires